Journal of Materials Science and Engineering A 16 (1-3) (2026) 41-46
doi: 10.17265/2161-6213/2026.1-3.005

Dynamically Tunable Anapole Metasurface Based on Silicon and Vanadium Dioxide

Cai Ju

Department of Physics, China Jiliang University, ZheJiang, Hangzhou 310018, China

Abstract: Metasurfaces have garnered extensive research attention owing to their exceptional capability for flexible manipulation of electromagnetic waves. Anapole modes and bound states in the continuum have become research hotspots in this field, due to their intrinsic non-radiating properties, ultra-high quality factor, and strong field enhancement effects. In this work, we propose a paired half-disk array hybrid metasurface based on silicon and vanadium dioxide, and systematically investigate the underlying physical mechanism of anapole resonance excitation via multipolar decomposition and electromagnetic field distribution analysis. Dynamic tuning of the anapole mode is successfully achieved by virtue of the insulator-metal phase transition of vanadium dioxide. By breaking the structural symmetry of the paired half-disks, we further realize the coexistence of anapole resonance and two symmetry-protected bound states in the continuum resonances, which is validated by band structure calculations. This work provides a novel design strategy for dynamically tunable ultra-high nanophotonic devices.

Key words: Vanadium dioxide, toroidal dipole, dielectric nanostructures, bound states in the continuum, anapole.

1. Introduction

Over the past decade, metasurfaces have garnered tremendous research attention owing to their exceptional capability to flexibly manipulate electromagnetic waves [1, 2]. Toroidal dipoles (TD) have attracted extensive interest for their intrinsic low-loss characteristics and ultra-high quality factor (Q-factor) [3-7]. The electric field distribution of a TD features two counter-rotating closed loops, which induce two anti-parallel magnetic dipole (MD) moments. These magnetic dipole moments connect end-to-end to form a closed toroidal configuration, which constitutes the most widely adopted design strategy for implementing TD in metasurfaces [8-10]. Existing studies on the application of TD generally focus on realizing TD resonances via dedicated metasurface design, and directly utilize the TD mode itself to generate electromagnetic resonances [11-13]. In contrast, an anapole can realize a dipole-moment-free electromagnetic response. It enables an electromagnetic interaction regime distinct from that of conventional materials by tailoring the electrical and magnetic properties of the constituent materials [14-19]. The emergence of the anapole state leverages the fundamental principle that the far-field radiation patterns of a TD and an electric dipole are identical in form, thus enabling complete destructive interference between the two dipole modes [20-22]. The realization of the anapole state in dielectric nanostructures is of profound significance for a broad spectrum of applications in nanophotonics [23-28]. However, conventional structural designs typically excite fundamental resonance modes dominated by electric and magnetic dipoles, resulting in a limited Q-factor and weak field enhancement [29-31]. Through rational metasurface engineering, the anapole state can be excited via the destructive interference between electric and toroidal dipoles, which can drastically boost the Q-factor of the resonance and the enhancement of the radiated field [32, 33].

In this work, we design a metasurface with a paired half-disk array that supports the anapole mode, and systematically investigate the underlying physical

Corresponding author: Cai Ju, master of science, research field: terahertz photonics.

mechanism of anapole resonance generation. Dynamic tuning of the anapole mode is achieved via the insulator-metal phase transition of vanadium dioxide. Subsequently, on the basis of the symmetric paired half-disk metasurface, we introduce an asymmetry factor by modifying the radius of one half-disk to break the structural symmetry, which enables the coexistence of the anapole mode and a symmetry-protected bound state in the continuum.

2. Results and Discussion

Fig. 1 (a) presents a schematic diagram of the proposed hybrid metasurface based on silicon and vanadium dioxide (VO_2). The metasurface consists of a periodic array of unit cells, each of which features a paired half-disk structure, where each half-disk is composed of a silicon layer with a VO_2 layer stacked on its top surface. As shown in Fig. 1(b), the two half-disks in the symmetric structure have identical radius is $r1 = r2 =$ 800 nm, where the silicon and VO_2 layers of each half-disk share the same radius. The metasurface exhibits periodicity along both the x and y axes, with a lattice constant P = 1,800 nm. Fig. 1(c) shows the side view of the unit cell, where the thickness of the top VO_2 layer is $h1$ = 20 nm, and the thickness of the underlying silicon layer is $h2$ = 600 nm. For x-polarized incident light, the transmission spectrum of the metasurface with VO_2 in its insulating phase features two resonances with distinct linewidths, as plotted by the black solid line in Fig. 1(d). The broad resonance is centered at 3,342 nm, while the narrow resonance is located at 3,829 nm, with a corresponding Q-factor of 240.1. When VO_2 undergoes the insulator-to-metal phase transition from the insulating phase to the metallic phase, as indicated by the red solid line in Fig. 1(d), the intensity of both resonances is significantly suppressed, and both resonance peaks exhibit a clear blue shift. This phenomenon is attributed to the dramatic increase in the imaginary part of the complex refractive index of VO_2 upon the phase transition.

To gain in-depth insight into the multipolar origin of the two observed resonances, we performed a systematic investigation via multipolar decomposition analysis. Fig. 2(a) presents the multipolar decomposition results for VO_2 in the insulating phase. At the broad resonance centered at 3,342 nm, the scattering power is predominantly dominated by the MD mode; in contrast, the TD mode contributes the overwhelming majority of the scattering power for the narrow resonance at 3,829 nm. To clarify the electromagnetic origin of the narrow resonance, we calculated the electromagnetic field distribution characteristics at the corresponding resonant frequency. Fig. 2(b) plots the electric field distribution of the narrow resonance at 3,829 nm. The electric field exhibits two counter-rotating closed loop configurations, and is strongly confined in the air gap

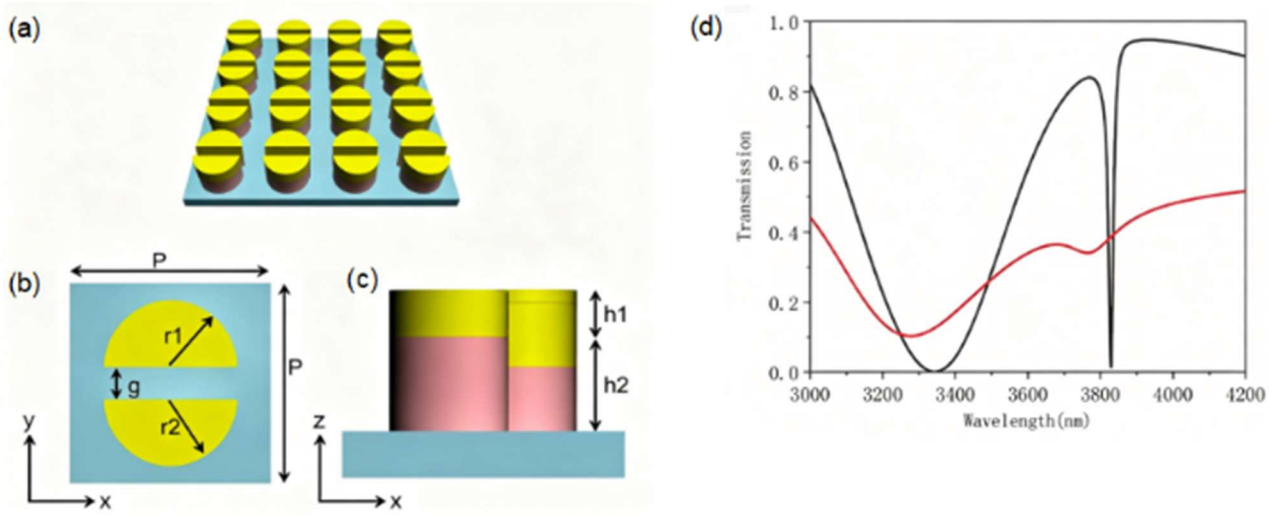

Fig. 1 Schematic illustration and transmission spectra of the paired half-disk structure.

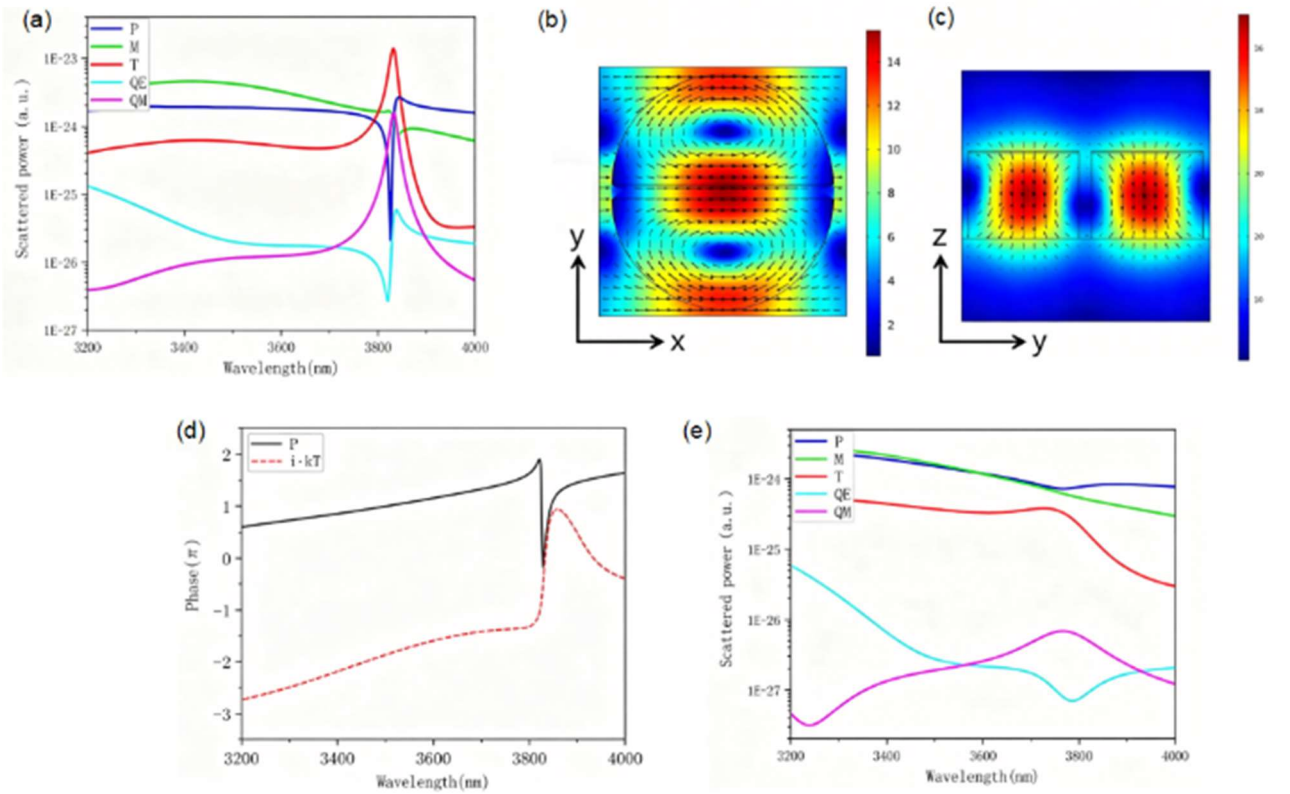

Fig. 2 Multipolar decomposition and electromagnetic field distribution profiles of the paired half-disk structure.

between the two dielectric structures. This field profile corresponds to an electric dipole (ED) resonance oriented along the positive x-direction. Fig. 2(c) shows the magnetic field distribution at 3,829 nm. The two counter-rotating closed loops of the electric field induce a head-to-tail closed magnetic field configuration, which forms a toroidal dipole. This field pattern corresponds to a toroidal dipole resonance oriented along the negative x-direction.

Subsequently, we calculated the phase distributions of the electric dipole and toroidal dipole moments. As shown in Fig. 2(d), we analyzed the phase of the electric dipole moment P and the term −ikT of the toroidal dipole moment. When the two phases are equal, the electric dipole and toroidal dipole exhibit opposite phases in the far-field radiation. By combining the multipolar decomposition and phase distribution results, it is confirmed that the electric dipole and toroidal dipole have equal amplitudes and opposite phases near the resonance frequency, which verifies the excitation of the anapole resonance at this spectral position. When VO_2 undergoes the phase transition to the metallic phase, the corresponding multipolar decomposition is calculated, as presented in Fig. 2(e). In this case, the resonance is dominated by the electric dipole mode, and the anapole state is completely quenched. These results demonstrate that dynamic tuning of the anapole resonance is successfully achieved via the insulator-to-metal phase transition of VO_2.

All the structures investigated in the aforementioned numerical simulations possess perfect structural symmetry. On the basis of the paired half-disk design, we modify the radius $r1$ of one half-disk to break the equality between $r1$ and $r2$, which disrupts the rotational symmetry of the structure and thereby excites symmetry-protected BIC resonances. With all other structural parameters fixed, the evolution of the transmission spectra with varying $r1$ is plotted in Fig. 3(a). Under the symmetric configuration, two resonances are present in the transmission spectrum. When the structural asymmetry is introduced, two new resonances emerge in the transmission spectrum, and their linewidth increases

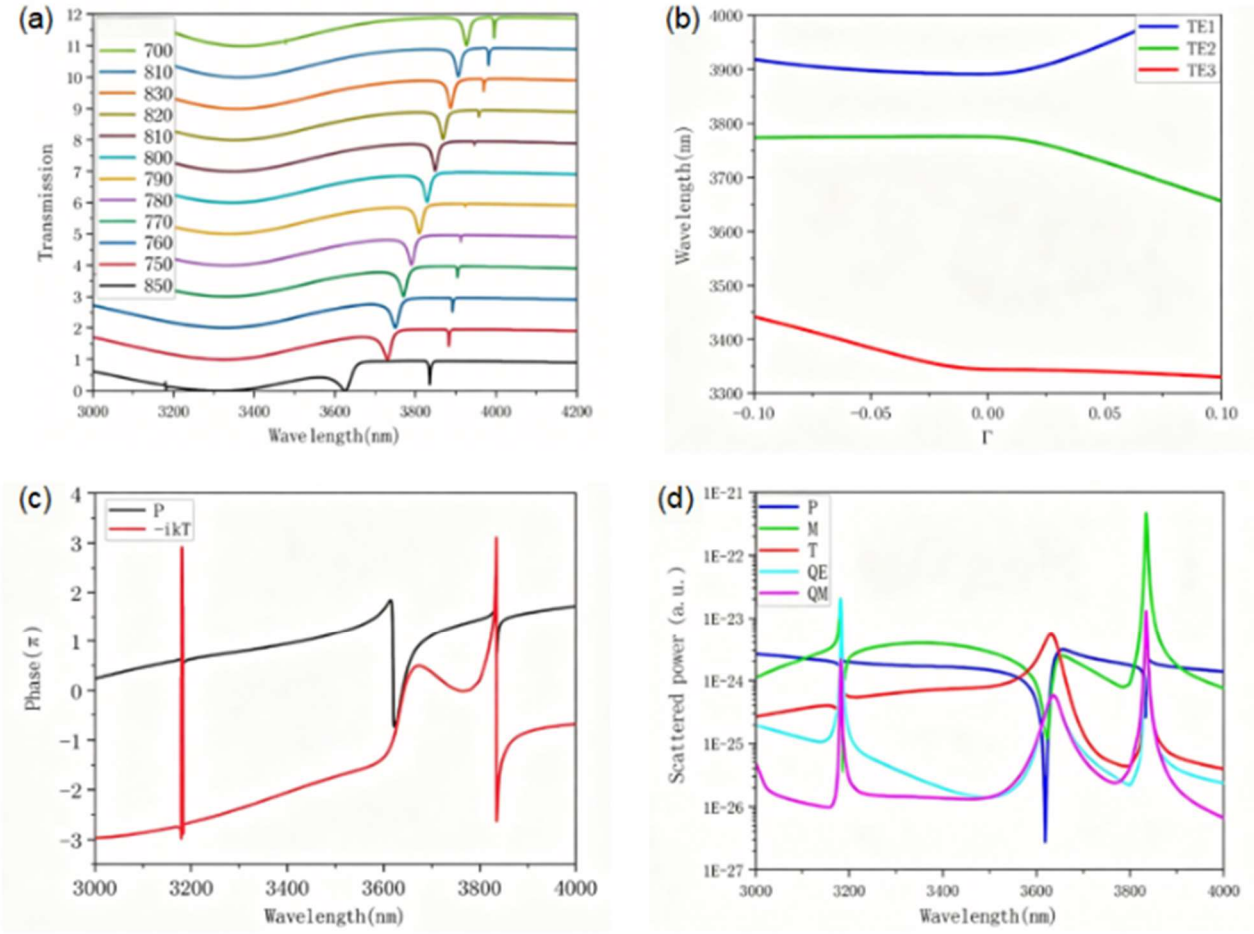

Fig. 3 Transmission spectra, BIC band structure diagrams, multipolar decomposition and phase distribution profiles of the paired half-disk structure with varying radius *r*1.

monotonically with the growing difference between *r*1 and *r*2. Two well-defined BIC resonances are clearly observed at *r*1 = 700 nm. To elucidate the origin of these newly emerged resonances, we performed multipolar decomposition analysis for the structure with *r*1 = 700 nm. The results of the multipolar decomposition and phase distribution are presented in Fig. 3(b). The first symmetry-protected BIC resonance is dominated by the electric quadrupole (EQ) mode, while the second symmetry-protected bound state in the continuum (BIC) resonance is predominantly contributed by the MD mode.

Notably, as shown in Fig. 3(c), the anapole resonance is still preserved in this asymmetric structure. At the wavelength of 3,646 nm, the electric dipole and toroidal dipole exhibit equal amplitudes and opposite phases, resulting in complete destructive interference and the formation of the anapole resonance. Consequently, the proposed asymmetric structure supports the coexistence of two symmetry-protected BIC resonances and one anapole resonance simultaneously.

Theoretically, every observable resonance in the transmission spectrum corresponds to a specific eigenmode in the band structure of the system. Accordingly, we calculated and analyzed the band structure characteristics of the paired half-disk metasurface. As illustrated in Fig. 3(d), the TE1 mode appears at the wavelength of 3,900 nm, which corresponds to the magnetic-dipole-mediated BIC resonance excited in the structure, with consistent electromagnetic field distribution and resonant position.

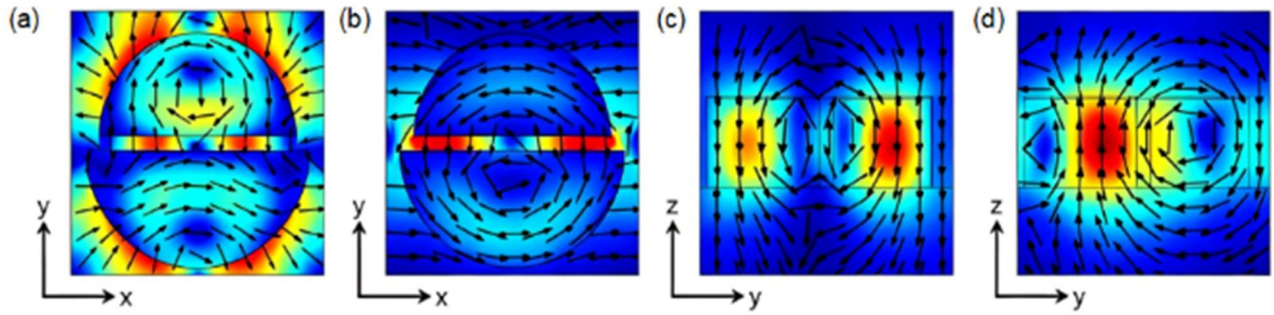

Fig. 4 Electromagnetic fields of the BIC resonance in the paired half-disk structure.

The TE2 mode corresponds to the anapole mode supported by the structure, while the TE3 mode matches the BIC resonance mode excited near 3,350 nm.

These two BIC resonances are dark modes, unobservable in the transmission spectrum when the structure is perfectly symmetric. Once the structural symmetry is broken, the BIC modes can couple with the free-space incident light, manifesting as two newly emerged resonances in the transmission spectrum. Our band structure analysis not only verifies the existence of the BIC modes, but also unambiguously identifies the exact spectral positions of the BIC resonances.

Subsequently, we calculated the electromagnetic field distributions of the two BIC resonances for the structure with $r1$ = 700 nm, as presented in Fig. 4(a) and Fig. 4(b). At the resonance wavelength of 3,181 nm, the electric fields in the two half-disks exhibit opposite orientations, which correspond to an EQ resonance. Meanwhile, the magnetic fields are uniformly aligned along the z-axis, which accounts for the non-negligible contribution of the MD mode observed in the multipolar decomposition results. Fig. 4(c) shows the electric field distribution at 3,834 nm, and Fig. 4(d) plots the electric field distribution in the y-z plane at the same wavelength. It can be seen from the field profiles that the electric field forms a closed loop configuration at 3,834 nm. According to the right-hand screw rule, this electric field distribution excites a magnetic dipole resonance oriented along the z-axis, confirming that this resonance is predominantly driven by the magnetic dipole mode.

4. Conclusions

We design a hybrid metasurface with a paired half-disk array based on silicon and VO_2, systematically investigate the excitation mechanism of the non-radiative anapole mode, realize active dynamic tuning of the anapole resonance via the insulator-metal phase transition of VO_2, and achieve the stable coexistence of the anapole mode and two symmetry-protected BIC in a single structure by introducing structural asymmetry to break the rotational symmetry of the metasurface. The relevant results are verified by multipolar decomposition, electromagnetic field distribution analysis and band structure calculation, which provide a new paradigm and theoretical support for the design of tunable high-Q nanophotonic devices.

References

[1] Chen, H.-T., Taylor, A. J., and Yu, N. 2016. “A Review of Metasurfaces: Physics and Applications.” *Rep. Prog. Phys.* 79: 076401.

[2] Brongersma, M. L., Pala, R. A., Altug, H., Capasso, F., Chen, W. T., and Majumdar, A. 2025. “The Second Optical Metasurface Revolution: Moving from Science to Technology.” *Nat. Rev. Electr. Eng.* 2: 125-43.

[3] Zel’Dovich, I. B. 1957. “Electromagnetic Interaction with Parity Violation.” *J. Exp. Theor. Phys*. 33: 1531-3.

[4] Guo, S., Talebi, N., Campos, A., et al. 2019. “Radiation of Dynamic Toroidal Moments.” *ACS photonics* 6 (2): 467-74.

[5] Dubovik, V. M., and Tosunyan, L. A. 1983. “Toroidal Moments in the Physics of Electromagnetic and Weak Interactions.” *Sov. J. Particles Nucl. (Engl. Transl.)* 14 (5).

[6] Wood, C. S., Bennett, S. C., Cho, D., et al. 1997. “Measurement of Parity Nonconservation and an Anapole Moment in Cesium.” *Science* 275 (5307): 1759-63.

[7] Spaldin, N. A., Fiebig, M., and Mostovoy, M. 2008. "The Toroidal Moment in Condensed-Matter Physics and its Relation to the Magnetoelectric Effect." *Journal of Physics: Condensed Matter* 20 (43): 434203.

[8] Basharin, A. A., Kafesaki, M., Economou, E. N., et al. 2015. "Dielectric Metamaterials with Toroidal Dipolar Response." *Physical Review X* 5 (1): 011036.

[9] Liu, S. D., Wang, Z. X., Wang, W. J., et al. 2017. "High Q-factor with the Excitation of Anapole Modes in Dielectric Split Nanodisk Arrays." *Optics Express* 25 (19): 22375-87.

[10] Tuz, V. R., Khardikov, V. V., and Kivshar, Y. S. 2018. "All-dielectric Resonant Metasurfaces with a Strong Toroidal Response." *Acs Photonics* 5 (5): 1871-6.

[11] Basharin, A. A., Chuguevsky, V., Volsky, N., et al. 2017. "Extremely High Q-factor Metamaterials due to Anapole Excitation." *Physical Review B* 95 (3): 035104.

[12] Yang, S., Liu, Z., Jin, L., et al. 2017. "Surface Plasmon Polariton Mediated Multiple Toroidal Resonances in 3D Folding Metamaterials." *Acs Photonics* 4 (11): 2650-8.

[13] Stenishchev, I. V., and Basharin, A. A. 2017. "Toroidal Response in All-Dielectric Metamaterials based on Water." *Scientific Reports* 7 (1): 9468.

[14] Chen, X., Wu, M., Liu, X., et al. 2019. "Tuning the Doping Ratio and Phase Transition Temperature of VO_2 Thin Film by Dual-Target Co-Sputtering." *Nanomaterials* 9 (6): 834.

[15] Atkin, J. M., Berweger, S., Chavez, E. K., et al. 2012. "Strain and Temperature Dependence of the Insulating Phases of VO_2 near the Metal-Insulator Transition." *Physical Review B* 85 (2): 020101.

[16] Hsu, C. W., Zhen, B., Stone, A. D., Joannopoulos, J. D. and Soljačić, M. 2016. "Bound States in the Continuum." *Nat. Rev. Mater.* 1: 1-13.

[17] Huang, L., Xu, L., Powell, D. A., Padilla, W. J., and Miroshnichenko, A. E. 2023. "Resonant Leaky Modes in All-Dielectric Metasystems: Fundamentals and Applications." *Phys. Rep.* 1008: 1-66.

[18] Wang, J., Li, P., Zhao, X., Qian, Z., Wang, X., Wang, F., Zhou, X., Han, D., Peng, C., Shi, L., and Zi, J. 2024. "Optical Bound States in the Continuum in Periodic Structures: Mechanisms, Effects, and Applications." *Photonics Insights* 3: 1-26.

[19] Tasolamprou, A. C., Tsilipakos, O., Kafesaki, M., et al. 2016. "Toroidal Eigenmodes in All-Dielectric Metamolecules." *Physical Review B* 94 (20): 205433.

[20] Gupta, M., Savinov, V., Xu, N., et al. 2016. "Sharp Toroidal Resonances in Planar Terahertz Metasurfaces." *Advanced Materials* 28 (37): 8206-11.

[21] Lv, W. Z., Wang, C., Zhang, D. Q., et al. 2024. "Switchable Multiple Quasibound States in the Continuum based on the Phase Transition of Vanadium Dioxide." *JOSA B* 41 (2): 432-41.

[22] Lv, T. T., Li, Y. X., Ma, H. F., et al. 2016. "Hybrid Metamaterial Switching for Manipulating Chirality based on VO_2 Phase Transition." *Scientific Reports* 6 (1): 23186.

[23] Nouman, M. T., Hwang, J. H., Faiyaz, M., et al. 2018. "Vanadium Dioxide based Frequency Tunable Metasurface Filters for Realizing Reconfigurable Terahertz Optical Phase and Polarization Control." *Optics Express* 26 (10): 12922-9.

[24] Zou, H., Xiao, Z., Li, W., et al. 2018. "Double-use Linear Polarization Convertor Using Hybrid Metamaterial based on VO_2 Phase Transition in the Terahertz Region." *Applied Physics A* 124 (4):322.

[25] Zhao, Y., Huang, Q., Cai, H., et al. 2018. "A Broadband and Switchable VO_2-based Perfect Absorber at the THz Frequency." *Optics Communications* 426: 443-9.

[26] Lv, T., Dong, G., Qin, C., et al. 2021. "Switchable Dual-band to Broadband Terahertz Metamaterial Absorber Incorporating a VO_2 Phase Transition." *Optics Express* 29 (4): 5437-47.

[27] Fang, N., Lee, H., Sun, C., et al. 2005. "Sub-Diffraction-Limited Optical Imaging with a Silver Superlens." *Science* 308 (5721): 534-537.

[28] Whittaker, L., Patridge, C. J., and Banerjee, S. 2011. "Microscopic and Nanoscale Perspective of the Metal−Insulator Phase Transitions of VO_2: Some New Twists to an Old Tale." *The Journal of Physical Chemistry Letters* 2 (7): 745-58.

[29] Kim, S. J., Lee, D., Chae, J. Y., et al. 2021. "Reconfigurable, Vivid Reflective Colors based on Solution-processed Fabry-Perot Absorber Using Thermochromic Vanadium Dioxide." *Applied Surface Science* 565: 150610.

[30] Li, J., Zhang, Y., Jin, R., et al. 2014. "Excitation of Plasmon Toroidal Mode at Optical Frequencies by Angle-resolved Reflection." *Optics Letters* 39 (23): 6683-6.

[31] Kaelberer, T., Fedotov, V. A., Papasimakis, N., et al. 2010. "Toroidal Dipolar Response in a Metamaterial." *Science* 330 (6010): 1510-2.

[32] Stenishchev, I. V., and Basharin, A. A. 2017. "Toroidal Response in All-dielectric Metamaterials based on Water." *Scientific Reports* 7 (1): 9468.

[33] Urban, M. J., Dutta, P. K., Wang, P., et al. 2016. "Plasmonic Toroidal Metamolecules Assembled by DNA Origami." *Journal of the American Chemical Society* 138 (17): 5495-8.